



A Glycosylphosphatidylinositol-Anchored α -Amylase Encoded by *amyD* Contributes to a Decrease in the Molecular Mass of Cell Wall α -1,3-Glucan in *Aspergillus nidulans*

OPEN ACCESS

Edited by:

Katherine A. Borkovich,
University of California, Riverside,
United States

Reviewed by:

Tuo Wang,
Louisiana State University,
United States
Stephen J. Free,
University at Buffalo, United States
Gerardo Díaz-Godínez,
Autonomous University of
Tlaxcala, Mexico

*Correspondence:

Keietsu Abe
keietsu.abe.b5@tohoku.ac.jp

Specialty section:

This article was submitted to
Fungal Physiology and Metabolism,
a section of the journal
Frontiers in Fungal Biology

Received: 25 November 2021

Accepted: 22 December 2021

Published: 28 January 2022

Citation:

Miyazawa K, Yamashita T, Takeuchi A,
Kamachi Y, Yoshimi A, Tashiro Y,
Koizumi A, Ogata M, Yano S,
Kasahara S, Sano M, Yamagata Y,
Nakajima T and Abe K (2022) A
Glycosylphosphatidylinositol-
Anchored α -Amylase Encoded by
amyD Contributes to a Decrease in
the Molecular Mass of Cell Wall
 α -1,3-Glucan in *Aspergillus nidulans*.
Front. Fungal Biol. 2:821946.
doi: 10.3389/ffunb.2021.821946

Ken Miyazawa^{1,2}, Takaaki Yamashita¹, Ayumu Takeuchi¹, Yuka Kamachi¹, Akira Yoshimi^{3,4}, Yuto Tashiro¹, Ami Koizumi¹, Makoto Ogata⁵, Shigekazu Yano⁶, Shin Kasahara⁷, Motoaki Sano⁸, Youhei Yamagata⁹, Tasuku Nakajima⁴ and Keietsu Abe^{1,4,10*}

¹Laboratory of Applied Microbiology, Department of Microbial Biotechnology, Graduate School of Agricultural Science, Tohoku University, Sendai, Japan, ²Laboratory of Filamentous Mycoses, Department of Fungal Infection, National Institute of Infectious Diseases, Tokyo, Japan, ³Laboratory of Environmental Interface Technology of Filamentous Fungi, Graduate School of Agriculture, Kyoto University, Kyoto, Japan, ⁴ABE-Project, New Industry Creation Hatchery Center, Tohoku University, Sendai, Japan, ⁵Faculty of Food and Agricultural Sciences, Fukushima University, Fukushima, Japan, ⁶Department of Biochemical Engineering, Graduate School of Engineering, Yamagata University, Yonezawa, Japan, ⁷Food Microbiology Unit, School of Food and Agricultural Sciences, Miyagi University, Sendai, Japan, ⁸Genome Biotechnology Laboratory, Kanazawa Institute of Technology, Hakusan, Japan, ⁹Department of Applied Life Science, The United Graduate School of Agricultural Science, Tokyo University of Agriculture and Technology, Fuchu, Japan, ¹⁰Department of Microbial Resources, Graduate School of Agricultural Science, Tohoku University, Sendai, Japan

α -1,3-Glucan is one of the main polysaccharides in the cell wall of *Aspergillus nidulans*. We previously revealed that it plays a role in hyphal aggregation in liquid culture, and that its molecular mass (MM) in an *agsA*-overexpressing (*agsA*^{OE}) strain was larger than that in an *agsB*-overexpressing (*agsB*^{OE}) strain. The mechanism that regulates its MM is poorly understood. Although the gene *amyD*, which encodes glycosylphosphatidylinositol (GPI)-anchored α -amylase (AmyD), is involved in the biosynthesis of α -1,3-glucan in *A. nidulans*, how it regulates this biosynthesis remains unclear. Here we constructed strains with disrupted *amyD* (Δ *amyD*) or overexpressed *amyD* (*amyD*^{OE}) in the genetic background of the ABPU1 (wild-type), *agsA*^{OE}, or *agsB*^{OE} strain, and characterized the chemical structure of α -1,3-glucans in the cell wall of each strain, focusing on their MM. The MM of α -1,3-glucan from the *agsB*^{OE} *amyD*^{OE} strain was smaller than that in the parental *agsB*^{OE} strain. In addition, the MM of α -1,3-glucan from the *agsA*^{OE} Δ *amyD* strain was greater than that in the *agsA*^{OE} strain. These results suggest that AmyD is involved in decreasing the MM of α -1,3-glucan. We also found that the C-terminal GPI-anchoring region is important for these functions.

Keywords: cell wall, filamentous fungi, *Aspergillus nidulans*, glycosylphosphatidylinositol-anchored protein, α -amylase, α -1,3-glucan

INTRODUCTION

The fungal cell wall, composed mainly of polysaccharides, is essential for the survival of the fungus (Latgè et al., 2017). It has recently been understood that the cell wall is a highly dynamic structure; cell-wall components are synthesized by synthases and then reconstructed by glycosyltransferases to form a proper cell-wall architecture (Latgè and Beauvais, 2014; Latgè et al., 2017). The cell wall of filamentous fungi contains α -glucans, β -glucans, chitin, and galactomannan. Some fungi form an extracellular matrix, which includes secretory polysaccharides such as galactosaminogalactan (Sheppard and Howell, 2016; Yoshimi et al., 2016; Miyazawa et al., 2019). Cell-wall polysaccharides of some *Aspergillus* species can be fractionated into alkali-soluble and alkali-insoluble fractions (Fontaine et al., 2000; Yoshimi et al., 2013; Dichtl et al., 2015; Zhang et al., 2017b). The alkali-soluble fraction contains mainly α -1,3-glucan with interconnecting α -1,4-linkage and some galactomannan (Bernard and Latge, 2001; Latgè, 2010). The alkali-insoluble fraction is composed of chitin, β -1,6-branched β -1,3-glucan, and galactomannan (Fontaine et al., 2000; Bernard and Latge, 2001). Recently, Kang et al. (2018) investigated the molecular architecture of the cell wall in *Aspergillus fumigatus* using solid-state NMR and suggested that the structure of the cell wall consists of a rigid inner domain and a highly mobile outer shell. Even more recently, Chakraborty et al. (2021) reported that α -1,3-glucan of *A. fumigatus* is present in both alkali-soluble and -insoluble fractions.

In the human pathogenic dimorphic yeast *Histoplasma capsulatum* and the rice blast fungus *Magnaporthe grisea*, α -1,3-glucan functions as a stealth factor that prevents host immune recognition and consequently contributes to the establishment of invasion or infection (Rappleye et al., 2004, 2007; Fujikawa et al., 2009, 2012). In addition, the pathogenesis of an α -1,3-glucan-deficient strain is decreased in murine models infected with *A. fumigatus* (Henry et al., 2012; Beauvais et al., 2013). Recently, α -1,3-glucan was reported to stimulate the polarization of regulatory T-cells by inducing programmed death-ligand 1 expression on human dendritic cells (Stephen-Victor et al., 2017). Fontaine et al. (2010) revealed that α -1,3-glucan has adhesivity when the conidia of *A. fumigatus* germinate.

Grün et al. (2005) analyzed the detailed chemical structure of α -glucan in the cell wall of the fission yeast *Schizosaccharomyces pombe* and found that its molecular mass (MM) is $42,600 \pm 5,200$, which is equivalent to a degree of polymerization of 263 ± 32 (Grün et al., 2005). The α -glucans derived from *S. pombe* are composed of two chains of ≈ 120 residues of 1,3-linked α -glucose with 12 residues of 1,4-linked α -glucose at the reducing ends (Grün et al., 2005). In *Aspergillus wentii*, the water-insoluble (alkali-soluble) glucan has a MM of $\approx 850,000$ and consists of 25 subunits (200 residues each) of α -1,3-glucan separated by short spacers composed of 1,4-linked α -glucan (Choma et al., 2013).

Aspergillus species have several α -1,3-glucan synthase genes: two in *Aspergillus nidulans* (*agsA* and *agsB*), three in *A. fumigatus* (*AGS1–3*) and *Aspergillus oryzae* (*agsA–C*), and five in *Aspergillus niger* (*agsA–E*). Disruptants of *A. fumigatus* that lack a single gene or all three genes have been constructed (Beauvais et al., 2005;

Maubon et al., 2006; Henry et al., 2012); these strains lack α -1,3-glucan in the cell wall and are less pathogenic (Beauvais et al., 2013). In *A. oryzae*, *agsB* (orthologous to *A. nidulans agsB*) is the primary α -1,3-glucan synthase gene (Zhang et al., 2017b). An *A. oryzae* disruptant lacking all three genes loses its cell-wall α -1,3-glucan and forms small hyphal pellets under liquid culture conditions (Miyazawa et al., 2016). In *A. niger*, the expression of *agsA* (orthologous to *A. fumigatus AGS3*; no ortholog in *A. nidulans*) and *agsE* (orthologous to *A. nidulans agsB*) is upregulated in the presence of stress-inducing compounds in the cell wall (Damveld et al., 2005). In the kuro (black) koji mold *Aspergillus luchuensis*, disruption of *agsE* (orthologous to *A. nidulans agsB*) improves the protoplast formation (Tokashiki et al., 2019). Recently Uechi et al. revealed that *A. luchuensis agsB* (no ortholog in *A. nidulans*) plays a role in nigeran synthesis (Uechi et al., 2021). In *A. nidulans*, α -1,3-glucan in vegetative hyphae is synthesized mainly by AgsB (Yoshimi et al., 2013; He et al., 2014). The hyphae of a mutant deficient in α -1,3-glucan became fully dispersed, showing that α -1,3-glucan is a hyphal aggregation factor (Yoshimi et al., 2013; He et al., 2014). We recently constructed strains overexpressing *agsA* (*agsA^{OE}*) and *agsB* (*agsB^{OE}*) in the genetic background of, respectively, *agsB* and *agsA* disruptants. The peak MM of alkali-soluble glucan from *agsA^{OE}* was $1,480,000 \pm 80,000$, which was four times that from the *agsB^{OE}* (MM, $372,000 \pm 47,000$) (Miyazawa et al., 2018). The alkali-soluble glucan derived from these strains contains several 1,4-linked spacer structures interlinking the α -1,3-glucan subunits, which each contain 200 glucose residues (Miyazawa et al., 2018).

Outside of *A. fumigatus*, *A. nidulans agsB* and its orthologs are clustered with two α -amylase-encoding genes (*amyD* and *amyG* in *A. nidulans*) (He et al., 2014; Yoshimi et al., 2017; Miyazawa et al., 2020). The *amyG* gene encodes an intracellular α -amylase and is crucial for α -1,3-glucan synthesis (He et al., 2014). The *amyD* gene in *A. nidulans* encodes glycosylphosphatidylinositol (GPI)-anchored α -amylase. He et al. (2014) reported that α -1,3-glucan contents increased by 50% in an *amyD*-disrupted (Δ *amyD*) strain and halved in an *amyD*-overexpressing (*actA(p)-amyD*) strain, suggesting that *amyD* has a repressive effect on α -1,3-glucan synthesis. In addition, He et al. (2017) analyzed the chronological changes of α -1,3-glucan contents under liquid culture conditions. Whereas, the amount of α -1,3-glucan in strains that overexpressed the α -1,3-glucanase-encoding gene (*mutA* or *agnB*) was decreased after 20 h from inoculation, the amount of α -1,3-glucan in the cell wall of the *amyD^{OE}* strain was half that of the wild-type strain from the initial stage of cultivation (He et al., 2017). He et al. (2017) suggested that AmyD decreased the amount of α -1,3-glucan in the cell wall by a mechanism independent of the effect of α -1,3-glucanase. The enzymatic characteristics of *A. niger* AgtA, which is encoded by an ortholog of *A. nidulans amyD*, have been reported (Van Der Kaaij et al., 2007). Although AgtA in *A. niger* barely hydrolyzed α -1,3-glucan, it had relatively high transglycosylation activity on donor substrates with maltooligosaccharides (Van Der Kaaij et al., 2007). Overall, AmyD seems to indirectly decrease the amount of α -1,3-glucan in the cell wall, but the detailed mechanism is still unknown.

TABLE 1 | Strains used in this study.

Strains	Genotype	References
A4		FGSC ^a
ABPU1 (<i>argB</i> ⁺) (wild-type)	<i>biA1, pyrG89, wA3, argB2, pyroA4, veA1, ligD::ptrA, AoargB</i> ⁺	Hagiwara et al., 2007; Miyazawa et al., 2018
Δ <i>amyD</i>	<i>biA1, pyrG89, wA3, argB2, pyroA4, veA1, ligD::ptrA, AoargB</i> ⁺ , <i>amyD::pyrG</i>	This study
<i>amyD</i> ^{OE}	<i>biA1, pyrG89, wA3, argB2, pyroA4, veA1, ligD::ptrA, AoargB</i> ⁺ , <i>Ptef1-amyD::pyrG</i>	This study
Δ <i>agsA</i>	<i>biA1, pyrG89, wA3, argB2, pyroA4, veA1, ligD::ptrA, AoargB</i> ⁺ , <i>agsA::loxP</i>	This study
<i>agsB</i> ^{OE}	<i>biA1, pyrG89, wA3, argB2, pyroA4, veA1, ligD::ptrA, AoargB</i> ⁺ , <i>agsA::loxP, Ptef1-agsB::pyroA</i>	This study
<i>agsB</i> ^{OE} Δ <i>amyD</i>	<i>biA1, pyrG89, wA3, argB2, pyroA4, veA1, ligD::ptrA, AoargB</i> ⁺ , <i>agsA::loxP, Ptef1-agsB::pyroA, amyD::pyrG</i>	This study
<i>agsB</i> ^{OE} <i>amyD</i> ^{OE}	<i>biA1, pyrG89, wA3, argB2, pyroA4, veA1, ligD::ptrA, AoargB</i> ⁺ , <i>agsA::loxP, Ptef1-agsB::pyroA, Ptef1-amyD::pyrG</i>	This study
Δ <i>agsB</i>	<i>biA1, pyrG89, wA3, argB2, pyroA4, veA1, ligD::ptrA, agsB::argB</i>	Yoshimi et al., 2013
<i>agsA</i> ^{OE}	<i>biA1, pyrG89, wA3, argB2, pyroA4, veA1, ligD::ptrA, agsB::argB, Ptef1-agsA::pyroA</i>	This study
<i>agsA</i> ^{OE} Δ <i>amyD</i>	<i>biA1, pyrG89, wA3, argB2, pyroA4, veA1, ligD::ptrA, agsB::argB, Ptef1-agsA::pyroA, amyD::pyrG</i>	This study
<i>agsA</i> ^{OE} <i>amyD</i> ^{OE}	<i>biA1, pyrG89, wA3, argB2, pyroA4, veA1, ligD::ptrA, agsB::argB, Ptef1-agsA::pyroA, Ptef1-amyD::pyrG</i>	This study
Δ <i>amyD-amyD</i> ^{OE}	<i>biA1, pyrG89, wA3, argB2, pyroA4, veA1, ligD::ptrA, AoargB</i> ⁺ , <i>amyD::pyrG, Ptef1-amyD::hph, pyrG</i> ⁻	This study
Δ <i>amyD-amyD</i> ^{OE} (Δ GPI)	<i>biA1, pyrG89, wA3, argB2, pyroA4, veA1, ligD::ptrA, AoargB</i> ⁺ , <i>amyD::pyrG, Ptef1-amyD(ΔGPI)::hph, pyrG</i> ⁻	This study
<i>agsB</i> ^{OE} Δ <i>amyD-amyD</i> ^{OE}	<i>biA1, pyrG89, wA3, argB2, pyroA4, veA1, ligD::ptrA, agsB::argB, Ptef1-agsA::pyroA, amyD::pyrG, Ptef1-amyD::hph, pyrG</i> ⁻	This study
<i>agsB</i> ^{OE} Δ <i>amyD-amyD</i> ^{OE} (Δ GPI)	<i>biA1, pyrG89, wA3, argB2, pyroA4, veA1, ligD::ptrA, agsB::argB, Ptef1-agsA::pyroA, amyD::pyrG, Ptef1-amyD(ΔGPI)::hph, pyrG</i> ⁻	This study

^aFungal Genetic Stock Center, USA.

Here, in a study of the function of *amyD* in α -1,3-glucan biosynthesis in *A. nidulans*, we constructed strains with overexpression or disruption of *amyD* in the genetic backgrounds of the wild-type, *agsA*^{OE}, and *agsB*^{OE}. We performed several chemical analyses of α -1,3-glucan derived from the strains, looking in particular at its MM, and examined the role of *amyD* in controlling the MM of α -1,3-glucan in the cell wall.

MATERIALS AND METHODS

Strains and Growth Media

Strains are listed in Table 1. Czapek-Dox (CD) medium was used as the standard culture, as described previously (Fujioka et al., 2007; Miyazawa et al., 2018).

Construction of the *agsA*- and *agsB*-Overexpressing Strains

We newly constructed *agsA*^{OE} and *agsB*^{OE} strains for this study. To generate *agsA*^{OE}, pAPyT-*agsA* plasmids (Miyazawa et al., 2018) were digested with *NotI* and transformed into a disrupted *agsB* (Δ *agsB*) strain (Supplementary Figure 1A). Correct integration of *agsA* overexpression cassettes was confirmed by PCR (Supplementary Figure 1B). To generate *agsB*^{OE}, the disrupted *agsA* (Δ *agsA*) strain was first generated using the *Cre/loxP* marker recycling system (Zhang et al., 2017a). The pAPG-*cre/DagsA* plasmid (Miyazawa et al., 2018) was

digested with *EcoRI* and transformed into the ABPU1 (*argB*⁺) strain. Candidate strains were selected on CD medium without uridine and uracil, and then cultured on CD medium with uridine and uracil and 1% xylose to induce *Cre* expression (Supplementary Figure 1C). Strains that required uridine and uracil were isolated, and then replacement of the *agsA* gene was confirmed by PCR (Supplementary Figure 1D). The pAPyT-*agsB* plasmid was digested with *NotI* and transformed into the Δ *agsA* strain (Supplementary Figure 1E). Correct integration of *agsB* overexpression cassettes was confirmed by PCR (Supplementary Figure 1B).

Construction of the *amyD*^{OE} Strain

The *amyD*^{OE} strain was constructed by replacing the native promoter with the constitutive *tef1* promoter. The sequences of the primers are listed in Supplementary Table 1. To generate *amyD*^{OE}, the plasmid pAPT-*amyD* was constructed (Supplementary Figure 2A). The 5'-non-coding region (amplicon 1) and the coding region (amplicon 2) of *amyD* were amplified from *A. nidulans* ABPU1 genomic DNA. The *pyrG* marker (amplicon 3) was amplified from the pAPG-*cre/DagsA* plasmid. The *tef1* promoter (amplicon 4) was amplified from the pAPyT-*agsB* plasmid. The four amplicons and a *SacI*-digested pUC19 vector were fused using an In-Fusion HD Cloning Kit (Clontech Laboratories, Inc., Mountain View, CA, USA). The resulting plasmid was digested with *SacI*, and

transformed into the ABPU1 (*argB*⁺), *agsA*^{OE}, and *agsB*^{OE} strains (Supplementary Figure 2B). Correct integration of the cassette was confirmed by PCR (Supplementary Figure 2C).

Disruption of the *amyD* Gene

In the first round of PCR, gene fragments containing the 5′-non-coding region (amplicon 1) and the coding region (amplicon 2) of *amyD* were amplified from ABPU1 genomic DNA, and the *pyrG* gene (amplicon 3) was amplified from *A. oryzae* genomic DNA (Supplementary Figure 2D). The three resulting fragments were gel-purified and fused into a disruption cassette in the second round of PCR. The resulting PCR product was gel-purified and transformed into the ABPU1 (*argB*⁺), *agsA*^{OE}, and *agsB*^{OE} strains (Supplementary Figure 2E). Replacement of the *amyD* gene was confirmed by PCR (Supplementary Figure 2F).

Expression of Complementary *amyD* Genes

The sequences of the primers are listed in Supplementary Table 1. A GPI-anchor modification site, the ω -site, was predicted with the GPI Prediction Server v. 3.0 (https://mendel.imp.ac.at/gpi/gpi_server.html), and the best score for the ω -site was Asn535 of AmyD. To remove the GPI anchor of AmyD, 54 nucleotides corresponding to the 18 amino acid residues from Asn535 in AmyD were deleted from the authentic *amyD* gene (Supplementary Figure 3A). To create complementary genes that have full-length open reading frames of either *amyD* or the gene without the GPI anchor-coding region, the plasmids pAHT-*amyD*, pAHdPT-*amyD*, pAHT-*amyD*(Δ GPI), and pAHdPT-*amyD*(Δ GPI) were first constructed (Supplementary Figure 3A). To construct pAHT-*amyD*, primers IF-Ptef1-hph-Fw and IF-*amyD*-up-hph-Rv were amplified by PCR using pAPT-*amyD* as a template (amplicon 1). The hygromycin-resistance gene *hph* (amplicon 2) was amplified with primers 397-5 and 397-3 from pSK397 (Krappmann et al., 2006). The two amplicons were fused using a NEBuilder HiFi DNA Assembly kit (New England Biolabs, Ipswich, MA, USA) according to the manufacturer's instructions. Then, to delete the GPI anchor-encoding region of *amyD*, PCR amplification was performed with primers ANamyD-dGPI-Fw and ANamyD-dGPI-Rv from the resulting pAHT-*amyD* plasmid with PrimeSTAR Max DNA Polymerase (Takara Bio Inc., Kusatsu, Japan). The amplified fragment was transformed into DH5 α competent cells, and the pAHT-*amyD*(Δ GPI) plasmid was obtained (Supplementary Figure 3A). To construct pAHdPT-*amyD*, the first half (amplicon 1) and the second half (amplicon 2) of *pyrG* were amplified from *A. oryzae* genomic DNA. The fragment containing *hph*, *tef1* promoter, and *amyD* (amplicon 3) was amplified from pAHT-*amyD*. The three amplicons were fused using a NEBuilder kit. For pAHdPT-*amyD*(Δ GPI) construction, the fragment containing *hph*, *tef1* promoter, and *amyD* lacking its GPI anchor-coding region (amplicon 3′) was amplified from pAHT-*amyD*(Δ GPI). The three amplicons and the *SacI*-digested pUC19 vector were fused using an In-Fusion HD Cloning Kit (Supplementary Figure 3B). The pAHdPT-*amyD* and pAHdPT-*amyD*(Δ GPI) plasmids were digested with *SacI* and transformed into the Δ *amyD* and *agsB*^{OE} Δ *amyD*

strains (Supplementary Figure 3C). Correct integration of the cassettes was confirmed by PCR (Supplementary Figure 3D).

RNA Extraction and Quantitative Real-Time PCR

Mycelial cells cultured in CD liquid medium for 24 h were collected, and total RNA was extracted from the cells by using Sepasol-RNA I Super G (Nakalai Tesque, Kyoto, Japan) in accordance with the manufacturer's instruction. The total RNA (2.5 μ g) was reverse-transcribed by using a SuperScript IV VILO Master Mix with ezDNase Enzyme (Invitrogen, Carlsbad, CA, United States). Quantitative real-time PCR was performed with a Mx3000P (Agilent Technologies, Santa Clara, CA, United States) with SYBR Green detection. For reaction mixture preparation, Thunderbird Next SYBR qPCR Mix (Toyobo Co., Ltd., Osaka, Japan) was used. Primers used for quantitative PCR are listed in Supplementary Table 1. An equivalent amount of cDNA, obtained from reverse transcription reactions using an equivalent amount of total RNA, was applied to each reaction mixture. The gene encoding histone H2B was used as a normalization reference (an internal control) for determining the target gene expression ratios.

Delipidization and Fractionation of Mycelial Cells

Cell walls were fractionated as previously described with some modification (Miyazawa et al., 2018). Mycelia cultured for 24 h in CD medium were collected by filtering through Miracloth (Merck Millipore, Darmstadt, Germany), washed with water, and freeze-dried. The mycelia were then pulverized in a MM400 bench-top mixer mill (Retch, Haan, Germany). The powder (1 g) was suspended in 25 mL of chloroform-methanol (3:1 vol/vol) and stirred at room temperature for 12 h to remove the total polar lipid content of the mycelial cells. The mixture was centrifuged (10,000 \times g, 10 min). The residue was suspended in chloroform-methanol, and the delipidizing procedure was repeated. Then the de-polar lipid residue was suspended in 40 mL of 0.1 M Na phosphate buffer (pH 7.0), and cell-wall components were fractionated by hot-water and alkali treatments, as described previously (Miyazawa et al., 2018). Hot-water-soluble, alkali-soluble, and alkali-insoluble fractions were obtained from this fractionation, and the alkali-soluble fraction was further separated into a fraction soluble in water at neutral pH (AS1) and an insoluble fraction (AS2). The monosaccharide composition of AS2 fractions was quantified according to Miyazawa et al. (2018).

To obtain mycelia cultured for 16 h, conidia (final conc. 5.0×10^5 /mL) were inoculated into 200 mL CD medium and rotated at 160 rpm at 37°C. The mycelia were collected and fractionated as described above.

¹³C NMR Analysis

The AS2 fraction of each strain (50 mg) was suspended in 1 mL of 1 M NaOH/D₂O and dissolved by vortexing. One drop of DMSO-d₆ (deuterated dimethyl sulfoxide) was then added to each fraction and the solutions were centrifuged (3,000 \times g, 5 min) to remove insoluble debris. ¹³C NMR spectra of the supernatants were obtained using a JNM-ECX400P spectrometer (JEOL,

Tokyo, Japan) at 400 MHz at 35°C (72,000 scans). Chemical shifts were recorded relative to the resonance of DMSO- d_6 .

Determination of the Average Molecular Mass of Alkali-Soluble Glucan

The MM of alkali-soluble glucan was determined by gel permeation chromatography (GPC) according to the methods of Puanglek et al. (2016), with some modification. A GPC-101 system (Showa Denko Co. Ltd., Tokyo, Japan) with an ERC-3125S degasser (Showa Denko) and an RI-71S refractive index detector (Showa Denko) was used for the measurement. It was fitted with a GPC KD-G 4A guard column (Showa Denko) and a GPC KD-805 column (8.0 × 300 mm; Showa Denko). The eluent was 20 mM LiCl in *N,N*-dimethylacetamide (DMAc), and the flow rate was 0.6 mL/min at 40°C. The detector was normalized with polystyrene standards (SM-105; Showa Denko). With SmartChrom software (Jasco, Tokyo, Japan), the GPC profile was divided into virtual time slices (n_i) with the height of each virtual slice from the base line (H_i) corresponding to a certain MM (M_i) obtained by calibrating the column. From these values, the number-average MM (M_n) and weight-average MM (M_w) were calculated as:

$$M_n = \frac{\sum H_i}{\sum (H_i/M_i)}$$

$$M_w = \frac{\sum (H_i \cdot M_i)}{\sum H_i}$$

Polydispersity was calculated as M_w/M_n .

Smith Degradation

Smith degradation of the alkali-soluble glucan was performed as described (Miyazawa et al., 2018). In brief, the AS2 fraction (20 mg) was suspended in 0.1 M acetate buffer (pH 3.9), oxidized with sodium periodate, reduced with sodium borohydride, hydrolyzed with trifluoroacetic acid, and freeze-dried. These procedures resulted in selective hydrolyzing of the 1,4-linked glucose residues, which contain vicinal hydroxyl groups, but not the 1,3-glucose residues in alkali-soluble glucan. The Smith-degraded sample was dissolved in DMAc containing LiCl for GPC analysis.

Fluorescent Labeling of Cell-Wall Polysaccharides

Mycelial cells cultured for 16 h in CD liquid medium were dropped on a glass slide and dried at 55°C for 15 min. The cells were fixed and labeled with α -1,3-glucan-binding domain-fused green fluorescent protein (AGBD-GFP) (Suyotha et al., 2013) for α -1,3-glucan, fluorophore-labeled antibody for β -1,3-glucan, and fluorophore-labeled lectin for chitin. The cells were then imaged by confocal scanning microscopy as described (Miyazawa et al., 2018). Enzymatic digestion of β -1,3-glucan in the hyphal cells was performed as described (Miyazawa et al., 2018).

Western Blotting

Culture broth in CD liquid medium incubated for 24 h was filtered through Miracloth. Proteins in the supernatant were precipitated with trichloroacetic acid, separated by SDS-PAGE,

and then transferred onto a polyvinylidene difluoride membrane. The membrane was blocked with the polyvinylidene difluoride blocking reagent for Can Get Signal (Toyobo). Antibodies of rabbit IgG against AmyD were developed with synthesized peptides (NH₂-C+SGERAGELDVPMSK-COOH) (Eurofins Genomics, Tokyo, Japan) and used as the primary antibody, diluted with Can Get Signal (Toyobo). Antibody binding was visualized using a horseradish peroxidase-conjugated goat anti-rabbit IgG secondary antibody (Pierce Biotechnology, Rockford, IL, USA) and an ImmunoStar LD chemiluminescent substrate (Fujifilm Wako Pure Chemical Corp., Osaka, Japan).

Assay for Glucosyltransferase Activity

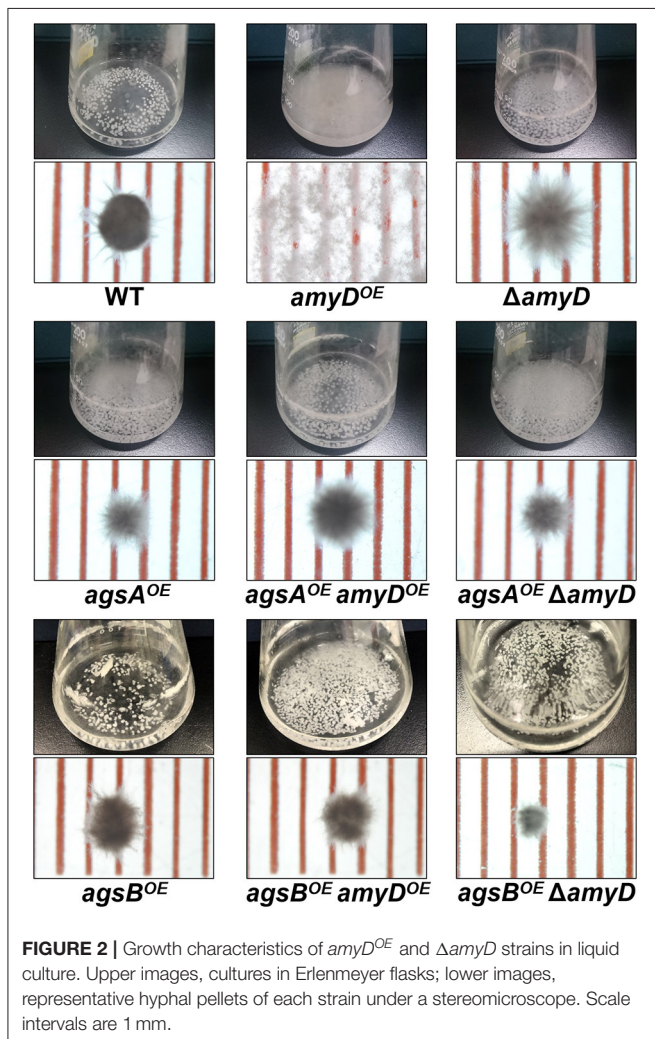
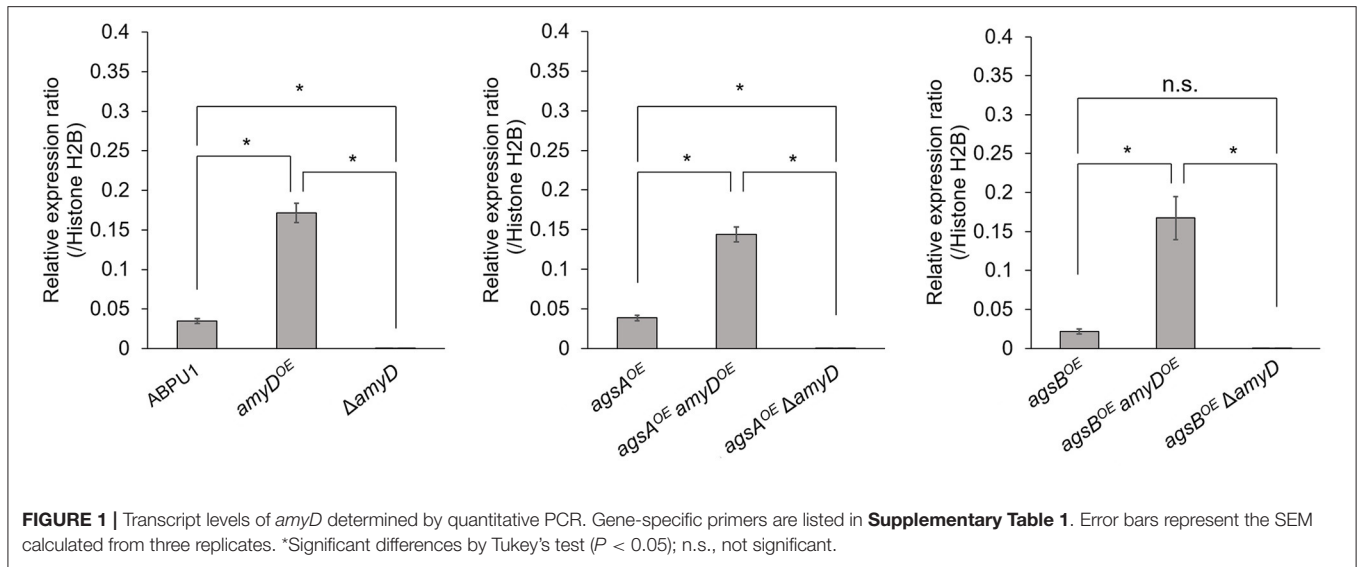
Supernatant obtained from CD liquid medium cultured for 24 h was concentrated 167 times and buffer-exchanged to 10 mM Tris-HCl (pH 8.0) in Nanosep Centrifugal Devices 10K (Pall, Port Washington, NY, USA). A 20- μ L mixture containing 1 mM *para*-nitrophenyl (*p*NP)- α -maltopentaoside and 1 mM acarbose (Fujifilm Wako Pure Chemical Corp.), and 5 μ L of the concentrated culture supernatant in 50 mM acetic acid/sodium acetate buffer (pH 5.5) was incubated for 20 min at 40°C. Samples (3 μ L) were withdrawn from the reaction mixture and immediately inactivated by adding 40 μ L of methanol. *p*NP- α -Maltopentaoside was prepared by following the method of Usui and Murata (1988). Then, 157 μ L of water was added to each sample solution, which was analyzed by HPLC with a Jasco Intelligent System liquid chromatograph (Jasco). The bound material was eluted with 20% methanol at a flow rate of 1.0 mL/min at 40°C. The elution profiles were detected at 300 nm with a Unison UK C-18 column (4.6 × 250 mm, Imtakt, Kyoto, Japan).

RESULTS

Characterization of Strains With Disrupted or Overexpressed *amyD*

We constructed *amyD*^{OE} and Δ *amyD* strains by introducing the *amyD* cassettes for overexpression and disruption into the wild-type, *agsA*^{OE}, and *agsB*^{OE} strains (Supplementary Figure 2). The expression level of *amyD* in each strain was quantified in hyphal cells. Whereas, each disrupted strain (Δ *amyD*, *agsA*^{OE} Δ *amyD*, and *agsB*^{OE} Δ *amyD*) showed scarce *amyD* expression, each overexpressing strain (*amyD*^{OE}, *agsA*^{OE} *amyD*^{OE}, and *agsB*^{OE} *amyD*^{OE}) showed significantly higher *amyD* expression than their parental strain (Figure 1).

There was no significant difference in radial growth among the strains grown on agar plates for 5 days (Supplementary Figure 4). In liquid culture, the wild-type and Δ *amyD* strains formed tightly aggregated hyphal pellets; however, the hyphae of the *amyD*^{OE} strain were almost fully dispersed (Figure 2). He et al. reported that the phenotype of their *amyD*^{OE} strain resembles that of the Δ *agsB* strain in *A. nidulans* (He et al., 2014), which is consistent with our results (Figure 2). In agreement with our previous results (Miyazawa et al., 2018), the *agsA*^{OE} and *agsB*^{OE} strains formed, respectively, loosely and tightly aggregated pellets (Figure 2). Disruption of *amyD* did not affect the phenotypes of the *agsA*^{OE} and



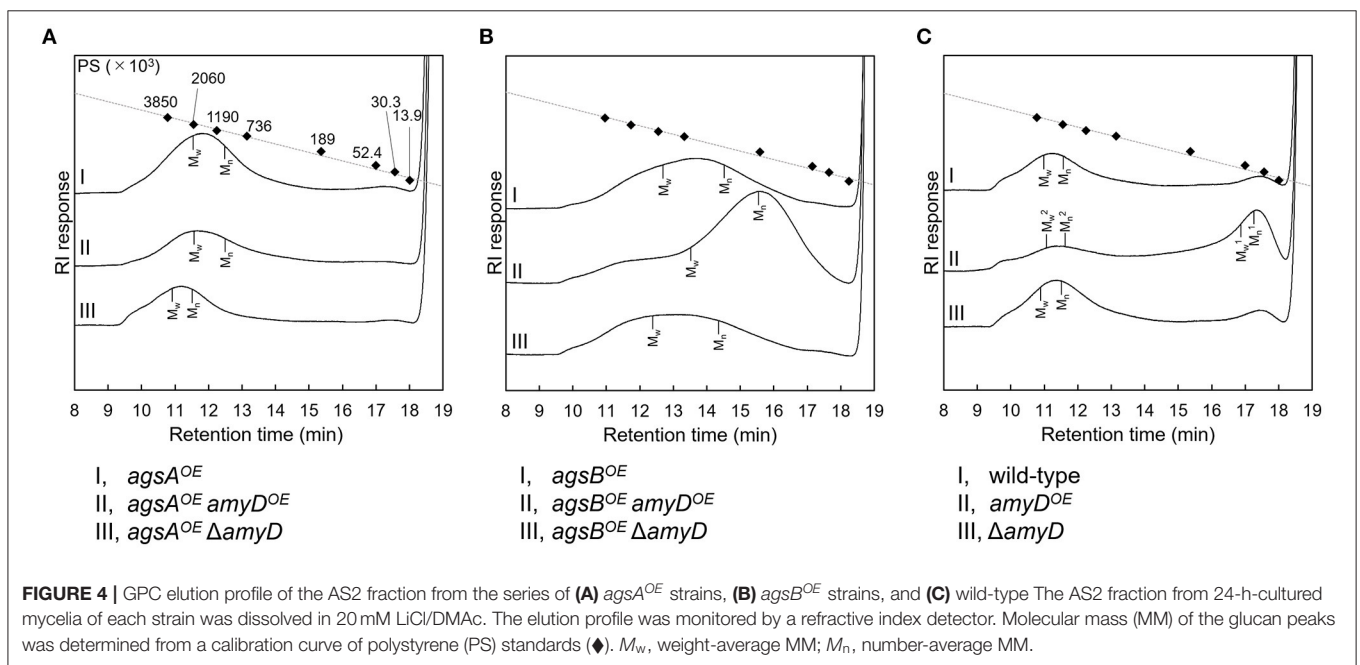
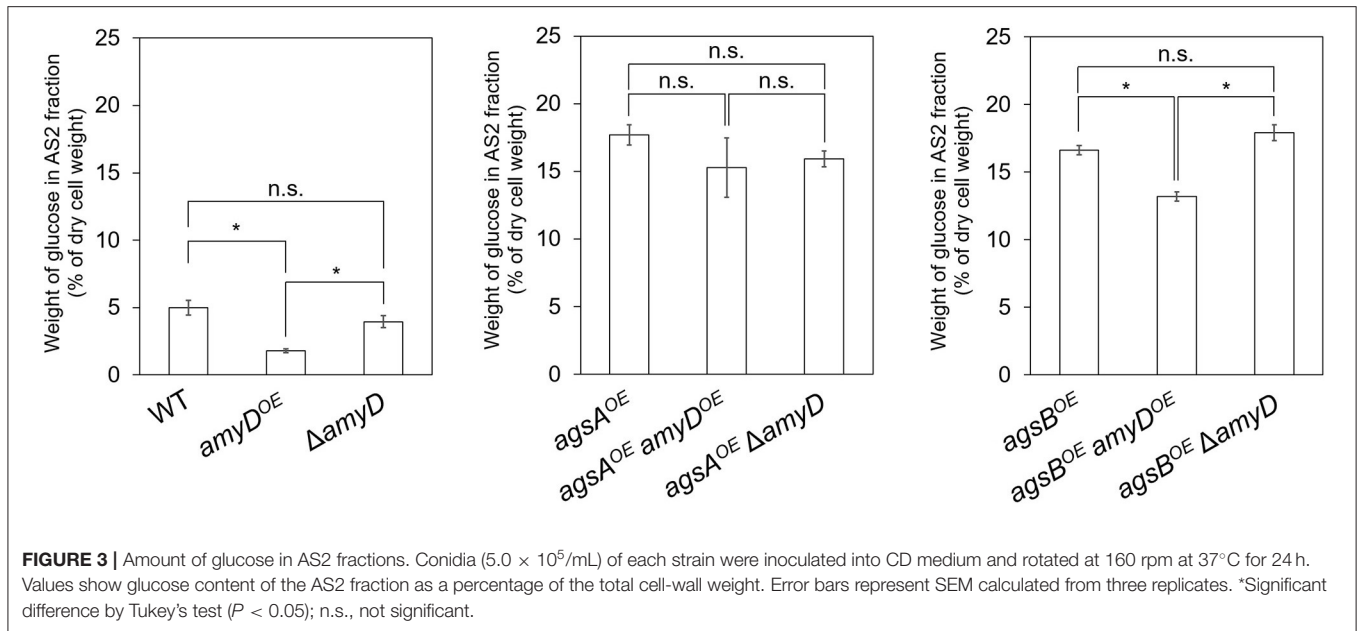
agsB^{OE} strains (**Figure 2**). Also, overexpression of *amyD* scarcely affected the phenotypes of the *agsA^{OE}* and *agsB^{OE}* strains (**Figure 2**).

Overexpression of *amyD* Resulted in a Decrease in Cell-Wall Alkali-Soluble Glucan

Cell-wall components of each strain were fractionated by a hot water-alkali treatment method, each fraction was weighed, and the monosaccharide composition of the AS2 fraction was quantified. The amount of glucose in the AS2 fraction was significantly lower in the *amyD^{OE}* strain than in the wild-type strain (**Figure 3**; $P < 0.05$). That in the Δ *amyD* strain was similar to that in the wild-type strain (**Figure 3**). Those in the *agsA^{OE}* *amyD^{OE}* and *agsA^{OE}* Δ *amyD* strains, which were constructed from the parental strain *agsA^{OE}*, were almost the same (**Figure 3**). It was significantly lower in the *agsB^{OE}* *amyD^{OE}* strain than in the *agsB^{OE}* and *agsB^{OE}* Δ *amyD* strains (**Figure 3**; $P < 0.05$). These results indicate that AmyD acts to decrease the amount of alkali-soluble glucan in the wild-type and *agsB^{OE}* strains, but not in the *agsA^{OE}* strain, even when *amyD* is overexpressed.

Overexpression of the *amyD* Gene Decreases the Molecular Mass of Alkali-Soluble Glucan

By ¹³C NMR analysis, the primary component in the AS2 fraction of the wild-type, *amyD^{OE}*, and Δ *amyD* strains was found to be α -1,3-glucan, suggesting that *amyD* did not affect the primary components of alkali-soluble glucan (**Supplementary Figure 5**). To reveal whether the MM of alkali-soluble glucan was affected by disruption or overexpression of *amyD*, we determined the MM of alkali-soluble glucan in each strain by GPC analysis. Polystyrene (MM, 13,900–3,850,000) was used as a standard molecule to calibrate the column for size exclusion analysis. Although M_w is used to assess the physical properties of a



polymer, the calculation of M_w favors molecules with a larger MM. Since M_n is the average of the MM values of the individual macromolecules, here we use M_n as the MM of alkali-soluble glucan. The M_n of the alkali-soluble glucan was $1,260,000 \pm 270,000$ in the *agsA*^{OE} strain and $312,000 \pm 5,000$ in *agsB*^{OE} strain (Figures 4A,B; Table 2), consistent with our previous results (Miyazawa et al., 2018). Although the M_n of alkali-soluble glucan in the *agsA*^{OE} *amyD*^{OE} strain ($1,110,000 \pm 110,000$) was similar to that in the parental (*agsA*^{OE}) strain, that of *agsA*^{OE} Δ *amyD* was significantly greater ($2,250,000 \pm 130,000$) than that of *agsA*^{OE} (Figure 4A; Table 2; $P < 0.05$). In addition, the

M_n of *agsB*^{OE} *amyD*^{OE} ($140,000 \pm 8,000$) was significantly less than that of the parental (*agsB*^{OE}) strain (Figure 4B; Table 2; $P < 0.05$). The M_n of alkali-soluble glucan in *agsB*^{OE} Δ *amyD* ($358,000 \pm 19,000$) was similar to that in *agsB*^{OE} (Figure 4B; Table 2). Lastly, the M_n of alkali-soluble glucan in the wild-type ($2,280,000 \pm 320,000$) and Δ *amyD* ($2,390,000 \pm 400,000$) was larger than that in *agsB*^{OE} ($312,000 \pm 5,000$; Figure 4C; Table 2). The *amyD*^{OE} strain had a primary peak at around 17 min (M_n^1 , $32,900 \pm 300$) and a secondary peak at 11 min (M_n^2 , $2,210,000 \pm 700,000$). These results suggest that AmyD degraded the alkali-soluble glucan eluted around 11 min to

TABLE 2 | Molecular mass of alkali-soluble glucan in the cell wall.

Sample	M_p^b	M_w^c	M_n^d	M_w/M_n
WT AS2 ^a	2,830,000 ± 400,000	3,510,000 ± 320,000	2,280,000 ± 320,000	1.55 ± 0.10
<i>amyD</i> ^{OE} AS2, peak 1	2,640,000 ± 400,000	3,350,000 ± 660,000	2,210,000 ± 700,000	1.57 ± 0.25
<i>amyD</i> ^{OE} AS2, peak 2	28,100 ± 1,100	41,600 ± 2,600	32,900 ± 300	1.30 ± 0.07
Δ <i>amyD</i> AS2	2,910,000 ± 270,000	3,540,000 ± 400,000	2,390,000 ± 400,000	1.49 ± 0.10
<i>agsA</i> ^{OE} AS2	1,930,000 ± 430,000	2,410,000 ± 240,000	1,260,000 ± 270,000	1.94 ± 0.20
<i>agsA</i> ^{OE} <i>amyD</i> ^{OE} AS2	2,000,000 ± 120,000	2,150,000 ± 170,000	1,110,000 ± 110,000	1.94 ± 0.05
<i>agsA</i> ^{OE} Δ <i>amyD</i> AS2	2,700,000 ± 300,000	3,380,000 ± 230,000	2,250,000 ± 130,000	1.50 ± 0.05
<i>agsB</i> ^{OE} AS2	623,000 ± 7,000	1,144,000 ± 13,000	312,000 ± 5,000	3.67 ± 0.03
<i>agsB</i> ^{OE} <i>amyD</i> ^{OE} AS2	169,000 ± 15,000	664,000 ± 14,000	140,000 ± 8,000	4.77 ± 0.16
<i>agsB</i> ^{OE} Δ <i>amyD</i> AS2	877,000 ± 91,000	1,435,000 ± 61,000	358,000 ± 19,000	4.01 ± 0.12

^aAS2, insoluble components after dialysis of the alkali-soluble fraction.

^bPeak molecular mass.

^cWeight-average molecular mass.

^dNumber-average molecular mass.

Values are mean ± standard deviation of three replicates.

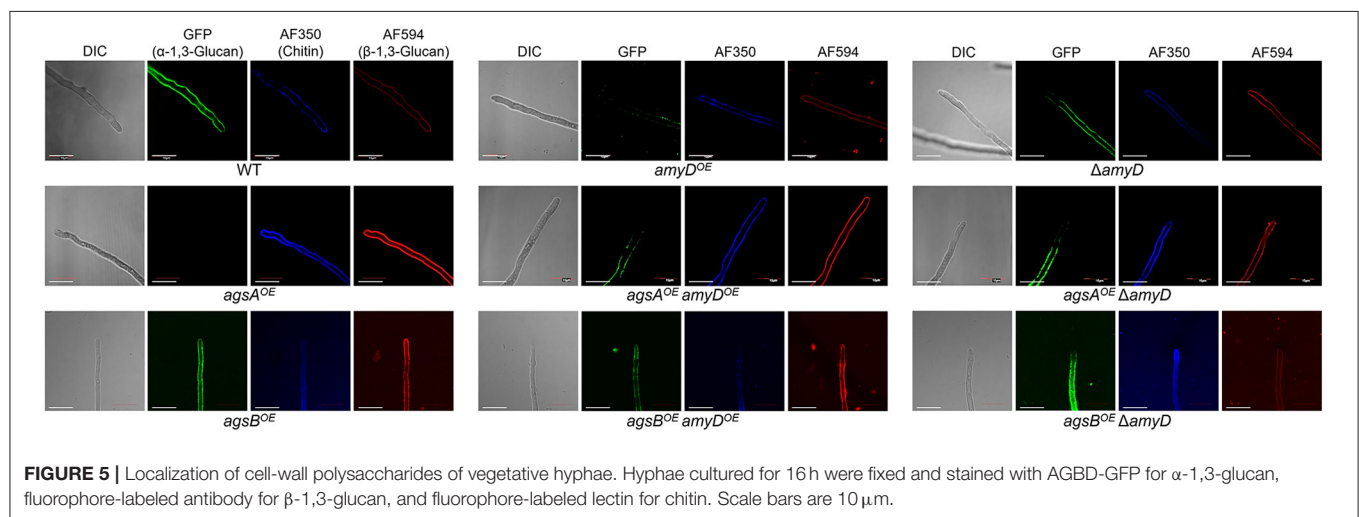


FIGURE 5 | Localization of cell-wall polysaccharides of vegetative hyphae. Hyphae cultured for 16 h were fixed and stained with AGBD-GFP for α -1,3-glucan, fluorophore-labeled antibody for β -1,3-glucan, and fluorophore-labeled lectin for chitin. Scale bars are 10 μ m.

produce alkali-soluble glucan with a smaller MM (**Figure 4C**; **Table 2**).

Although the alkali-soluble glucan in the wild-type strains was synthesized mainly by AgsB, its MM was larger than that in the *agsB*^{OE} strain (**Table 2**). Additionally, when *agsB* was overexpressed, the amount of α -1,3-glucan was three times that in the wild-type (**Figure 3**). We supposed that some unknown glycosyl modification enzymes may contribute to the increase in MM of α -1,3-glucan in the wild-type, and that because the *agsB*^{OE} strain produces more α -1,3-glucan, there is little modification by the unknown enzymes. Therefore, we determined the MM of alkali-soluble glucan extracted from 16-h cultured mycelia, which should be less affected by the modification enzyme than the 24-h cultured mycelia (He et al., 2017). Unexpectedly, the M_n of the alkali-soluble glucan in the mycelia cultured for 16 h was 1,980,000 ± 320,000, which was similar to that in the mycelia cultured for 24 h (1,930,000 ± 280,000; **Supplementary Figure 6**; **Supplementary Table 2**). We then evaluated the MM of

alkali-soluble glucan in A4, which is the Glasgow wild-type of *A. nidulans* (**Table 1**), and found it had $M_n = 2,224,000 \pm 390,000$ (**Supplementary Table 3**), which is similar to that in the wild-type strain.

To validate whether the degree of polymerization of α -1,3-glucan subunits in the alkali-soluble glucan was altered when the MM was changed by *amyD* disruption or overexpression, we applied Smith degradation to the alkali-soluble glucan from each strain to selectively cleave 1,4-linked glucan, and then determined the MM by GPC. One subunit of α -1,3-glucan in the alkali-soluble glucan is composed of ≈ 200 glucose residues (Choma et al., 2013; Miyazawa et al., 2018). The Smith-degraded alkali-soluble glucan in each strain had almost the same MM, equivalent to 300–400 glucose residues (**Supplementary Figure 7**; **Supplementary Table 4**), which suggests that AmyD activity does not decrease the degree of polymerization of the glucose residues in each α -1,3-glucan subunit.

Spatial Localization of α -1,3-Glucan in the Cell Wall Is Not Affected by *amyD* Disruption or Overexpression

We previously revealed that spatial localization of α -1,3-glucan in the cell wall changes according to its MM (Miyazawa et al., 2018); α -1,3-glucans in *agsB^{OE}* cells are localized in the outer layer in the cell wall, whereas most of those in the *agsA^{OE}* cells are masked by a β -1,3-glucan layer. In this study, disruption or overexpression of *amyD* altered the MM of alkali-soluble glucan (Figure 4; Table 2); therefore, we analyzed whether this alteration affected the spatial localization of α -1,3-glucan in the cell wall. In agreement with previous results (Miyazawa et al., 2018), the α -1,3-glucans with AGBD-GFP labeling showed clearly in the wild-type and *agsB^{OE}* cells, but only weakly in *agsA^{OE}* cells (Figure 5). The Δ *amyD* and *amyD^{OE}* cells were also labeled with AGBD-GFP (Figure 5); fluorescent intensity in *amyD^{OE}* was relatively low, which might be caused by a decrease in the amount of alkali-soluble glucan in the cell wall of *amyD^{OE}* cells. The labeling with AGBD-GFP in *agsA^{OE} amyD^{OE}* and *agsA^{OE} Δ amyD* cells was weak, as was that in the cells of the parental *agsA^{OE}* strain (Figure 5). The *agsB^{OE} Δ amyD* cells were clearly labeled with AGBD-GFP, as in the parental *agsB^{OE}* (Figure 5). The AGBD-GFP labeling was slightly weaker in *agsB^{OE} amyD^{OE}* than in *agsB^{OE}*, which might be attributable to a decrease in the amount of α -1,3-glucan. After treatment with β -1,3-glucanase, α -1,3-glucans of the hyphal cells in *agsA^{OE}*, *agsA^{OE} amyD^{OE}*, and *agsA^{OE} Δ amyD* cells were clearly labeled with AGBD-GFP (Supplementary Figure 8), suggesting that these strains have α -1,3-glucan in the inner layer of the cell wall in their hyphal cells. Taken together, these findings indicate that disruption or overexpression of *amyD* gene scarcely affected the spatial localization of α -1,3-glucan in the cell wall.

The GPI Anchor Is Essential for the Effect of AmyD on Both the Amount and Molecular Mass of Alkali-Soluble Glucan

AmyD is thought to contain a GPI anchor at the C-terminal region. Fungal GPI anchor-type proteins are transferred from the plasma membrane to the cell wall by the activity of the GH76 family (Vogt et al., 2020). We speculated that localization in the cell wall would be essential for AmyD to reach the substrate, alkali-soluble glucan, so we constructed overexpression strains of *amyD* with and without the GPI-anchor site. Because we noticed that overexpression of *amyD* alters the phenotype or the alkali-soluble glucan, we used Δ *amyD* and *agsB^{OE} Δ amyD* strains as hosts for the *amyD^{OE}* strains. The hyphae of Δ *amyD* formed pellets in shake-flask culture (Figure 6). Those of Δ *amyD-amyD^{OE}* were dispersed, as in *amyD^{OE}* (Figure 6). Those of Δ *amyD-amyD^{OE}(Δ GPI)* formed pellets, although the form was slightly different from that in the parental strain (Figure 6). Those of *agsB^{OE} Δ amyD*, *agsB^{OE} Δ amyD-amyD^{OE}*, and *agsB^{OE} Δ amyD-amyD^{OE}(Δ GPI)* formed similar pellets (Figure 6). Although the Δ *amyD-amyD^{OE}* hyphae had less AS2-Glc (1.13% \pm 0.21%) than Δ *amyD* (5.68% \pm 0.25%), the amount was restored in Δ *amyD-amyD^{OE}(Δ GPI)* hyphae (5.17% \pm 0.46%; Figure 7A). These results suggest that

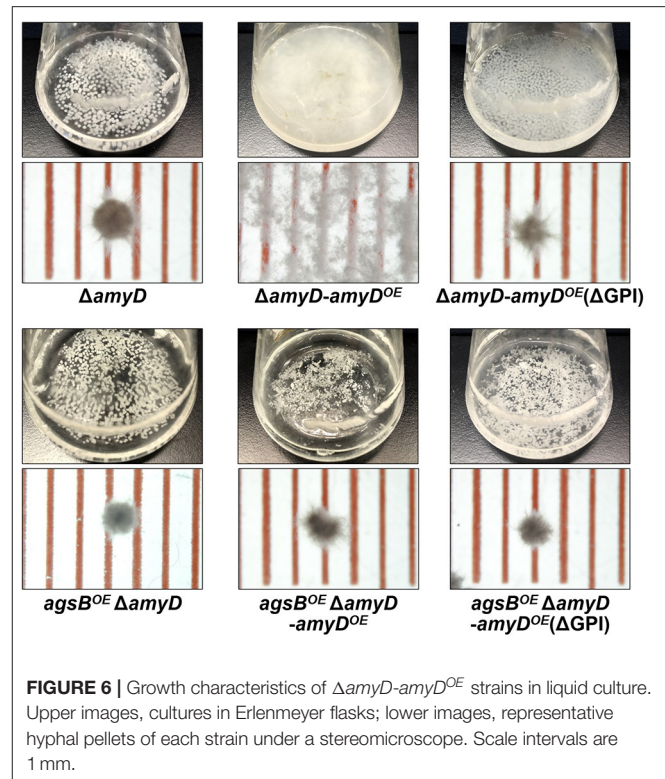
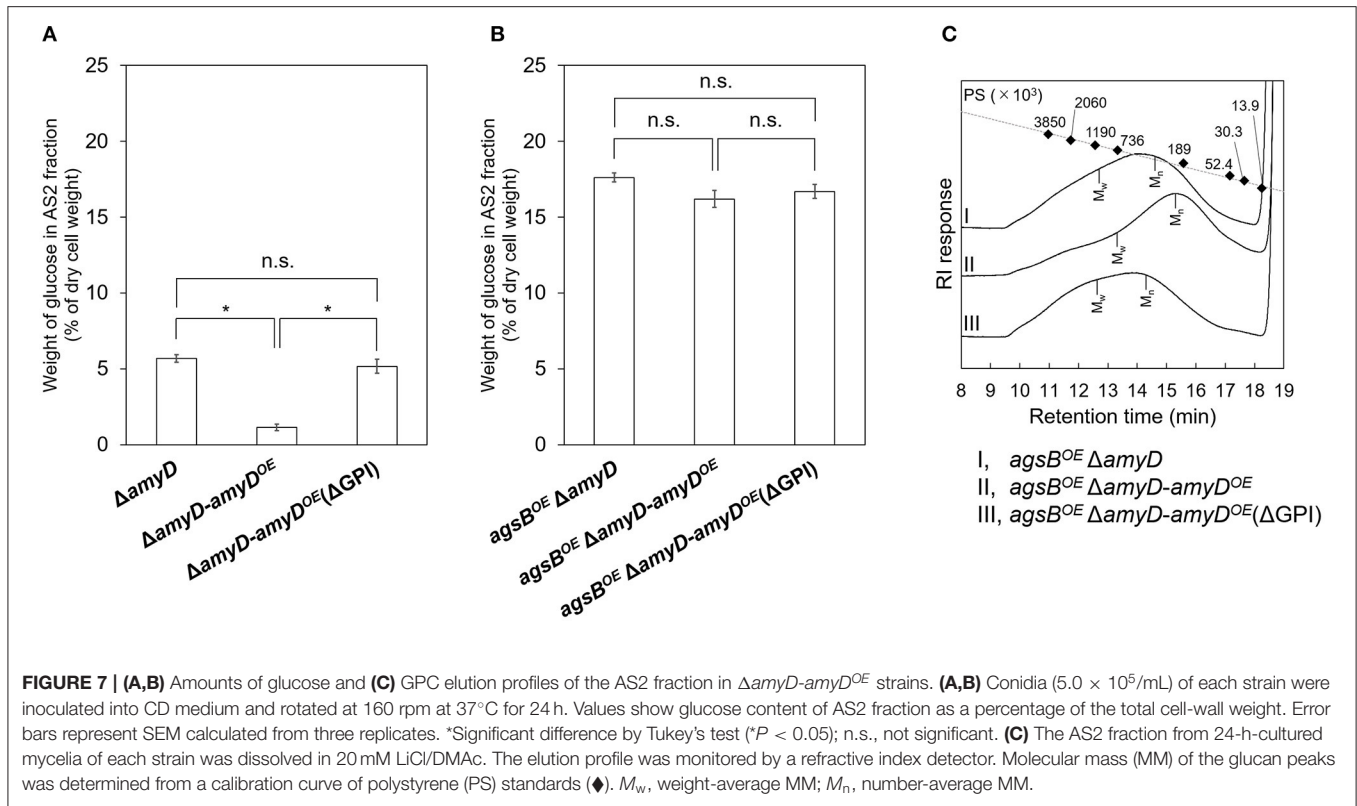


FIGURE 6 | Growth characteristics of Δ *amyD-amyD^{OE}* strains in liquid culture. Upper images, cultures in Erlenmeyer flasks; lower images, representative hyphal pellets of each strain under a stereomicroscope. Scale intervals are 1 mm.

the GPI anchor of AmyD has an important negative effect on α -1,3-glucan biosynthesis. The hyphae of *agsB^{OE} Δ amyD-amyD^{OE}* had marginally less AS2-Glc (16.2% \pm 0.6%) than those of *agsB^{OE} Δ amyD* (17.6% \pm 0.3%) and *agsB^{OE} Δ amyD-amyD^{OE}(Δ GPI)* (16.7% \pm 0.5%; Figure 7B). We then evaluated the MM of alkali-soluble glucan in the cells of *agsB^{OE} Δ amyD*, *agsB^{OE} Δ amyD-amyD^{OE}*, and *agsB^{OE} Δ amyD-amyD^{OE}(Δ GPI)*. The M_n of the alkali-soluble glucan in *agsB^{OE} Δ amyD-amyD^{OE}* cells (174,000 \pm 8,000) was smaller than that in *agsB^{OE} Δ amyD* (270,000 \pm 8,000; Figure 7C; Table 3; $P < 0.05$). The M_n of alkali-soluble glucan in *agsB^{OE} Δ amyD-amyD^{OE}(Δ GPI)* cells (349,000 \pm 42,000) was similar to that in *agsB^{OE} Δ amyD* (Figure 7C; Table 3). These results suggest that the GPI anchor of AmyD is also important for regulating the MM of alkali-soluble glucan.

Western blotting showed that secretion of AmyD in the culture supernatant could be detected only in the Δ *amyD-amyD^{OE} (Δ GPI)* strain (Supplementary Figure 9A). Because AgtA in *A. niger* has relatively high transglycosylation activity on donor substrates with maltooligosaccharides (Van Der Kaaij et al., 2007), we evaluated the α -amylase activity in concentrated culture supernatants with *p*NP- α -maltopentaoside. Although various products possibly produced by coexisting α -glucosidase were detected in Δ *amyD* and both *amyD*-overexpressing strains, *p*NP- α -maltooctaoside (probably a transglycosylation product of AmyD) was detected only in the Δ *amyD-amyD^{OE} (Δ GPI)* strain (data not shown). A histidine residue in region I, which is a highly conserved region of α -amylases, is substituted to the asparagine residue in AmyD and proteins encoded by orthologs of *amyD* (Van Der Kaaij et al., 2007). Substitution

**TABLE 3 |** Molecular mass of alkali-soluble glucan in the cell wall of $\Delta amyD$ - $amyD^{OE}$ strains.

Sample	M_p^b	M_w^c	M_n^d	M_w/M_n
$agsB^{OE} \Delta amyD$ AS2 ^a	391,000 ± 68,000	1,107,000 ± 47,000	270,000 ± 8,000	4.11 ± 0.29
$agsB^{OE} \Delta amyD$ - $amyD^{OE}$ AS2	220,000 ± 19,000	742,000 ± 107,000	174,000 ± 8,000	4.25 ± 0.44
$agsB^{OE} \Delta amyD$ - $amyD^{OE}$ (ΔGPI) AS2	807,000 ± 233,000	1,450,000 ± 128,000	349,000 ± 42,000	4.16 ± 0.14

^aAS2, insoluble components after dialysis of the alkali-soluble fraction.^bPeak molecular mass.^cWeight-average molecular mass.^dNumber-average molecular mass.

Values are mean ± standard deviation of three replicates.

of the histidine residues in α -amylase increases the inhibitory constant (K_i) of a representative α -glucosidase inhibitor, acarbose (Svensson, 1994). Therefore, we evaluated the α -amylase activity in concentrated culture supernatants in the presence of acarbose. As expected, the hydrolysis product of pNP - α -maltopentaoside was hardly detected in $\Delta amyD$ (Supplementary Figure 9B). pNP - α -maltoside and pNP - α -maltooctaoside were clearly detected in the supernatant of $\Delta amyD$ - $amyD^{OE}$ (ΔGPI), but scarcely in that of $\Delta amyD$ - $amyD^{OE}$ (Supplementary Figure 9B). These results suggest that although enzymatically active AmyD is secreted into the culture supernatant, it cannot decrease the MM of α -1,3-glucan, leading us to suppose that active AmyD needs to be localized on the plasma membrane or in the cell wall space to regulate the MM of α -1,3-glucan.

DISCUSSION

Although the GPI-anchored α -amylase AmyD is known to be involved in the biosynthesis of α -1,3-glucan in *A. nidulans* (He et al., 2014, 2017), the detailed mechanism remains unclear. Here, we looked at strains with disrupted or overexpressed $amyD$ to analyze how AmyD affects the chemical properties of alkali-soluble glucan. The results reveal that overexpression of $amyD$ not only decreased the MM of α -1,3-glucan, but also decreased the amount of α -1,3-glucan in the cell wall. The GPI anchor of AmyD was essential in both actions.

Overexpression of $amyD$ affected the amount and MM of α -1,3-glucan in the wild-type and $agsB^{OE}$ strains, but not in the $agsA^{OE}$ strain (Figures 3, 4; Table 2). We previously reported that the MM of α -1,3-glucan controls where α -1,3-glucan is

localized in the cell wall of *A. nidulans*; namely, that the α -1,3-glucan with a larger MM that is synthesized by AgsA is localized in the inner layer of the cell wall, and the smaller one that is synthesized by AgsB is localized in the outer layer (Miyazawa et al., 2018). To explain the effect of AmyD on the amount and MM of α -1,3-glucan, we formed the following two hypotheses from the results of this study. (1) Given that fungal GPI-anchored proteins are transferred from the plasma membrane to the cell wall (Orlean, 2012; Gow et al., 2017), our findings suggest that AmyD decreased the MM of α -1,3-glucan localized at the outer layer of the cell wall. The increased MM of alkali-soluble glucan in the *agsA*^{OE} Δ *amyD* strain can be explained by its GPC elution profiles, which suggest that the MM of the polysaccharides was broadly distributed (Figure 4A); in other words, *agsA*^{OE} Δ *amyD* had mainly α -1,3-glucan with larger MM [$>623,000$ (M_p of alkali-soluble glucan from *agsB*^{OE}), 97.5%], but also had a small amount of α -1,3-glucan with small MM ($<623,000$, 2.5%). We speculate that this small amount of α -1,3-glucan with a smaller MM may be localized in the outer layer of the cell wall of *agsA*^{OE}, where it is accessible to AmyD, which results in the small amount of α -1,3-glucan with a smaller MM. (2) Generally, as the degree of polymerization increases, the solubility of polysaccharides in water decreases (Guo et al., 2017). We have previously explained that after the biosynthesis of α -1,3-glucan on the plasma membrane, sugar chains are released to the outside of the membrane, where they are gradually insolubilized and immobilized to become a part of the cell wall (Miyazawa et al., 2018). Because α -1,3-glucan molecules with a larger MM might be more quickly insolubilized than those with a smaller MM, they are consequently localized in the inner layer of the cell wall, whereas α -1,3-glucan with a smaller MM might more likely be distributed toward the outer layer of the cell wall. α -1,3-Glucan synthesized with smaller MM in the *agsB*^{OE} strain, which takes a relatively long time to become insoluble, seems to be more catalytically accessible by AmyD than α -1,3-glucan synthesized with larger MM in the *agsA*^{OE} strain. To understand the relationship between the spatial localization of AmyD and α -1,3-glucan in the cell wall, immunoelectron microscopic and glycochemical analyses are necessary and are our future work.

AmyD of *A. nidulans* is considered to be a GPI-anchored protein (De Groot et al., 2009; He et al., 2014). It is well-known that many fungal GPI-anchored proteins are related to remodeling of the cell wall (Samalova et al., 2020). Proteins in the “defective in filamentous growth” (DFG) family recognize the GPI core glycan and then transfer to the β -1,3- or β -1,6-glucan (Muszkieta et al., 2019; Vogt et al., 2020), which allows GPI-anchored proteins to react with their substrates in the cell wall. Although there is no direct evidence that DFG family proteins contribute to transglycosylation in *Aspergillus* species, their role in cell-wall integrity in *A. fumigatus* was recently reported (Li et al., 2018; Muszkieta et al., 2019), which implies that DFG family proteins are important for transferring the GPI-core glycan to β -glucan in *Aspergillus* species. To reveal the importance of the GPI anchor in the function of AmyD, we evaluated the MM and amount of α -1,3-glucan in *amyD*-overexpressing strains with or without the GPI-anchoring site. Interestingly, decreases in the MM and the amount of

α -1,3-glucan were not observed when the C-terminal GPI-anchoring site was deleted (Figure 7; Table 3); Δ *amyD-amyD*^{OE} (Δ GPI) formed slightly altered pellets (Figure 6), suggesting that AmyD expressed without its GPI anchor has only partial functions. Furthermore, western blotting detected the secretion of AmyD in the culture supernatant from the Δ *amyD-amyD*^{OE} (Δ GPI) strain (Supplementary Figure 9A). AgtA in *A. niger* has relatively high glucosyltransferase activity toward donor substrates with maltooligosaccharides (Van Der Kaaij et al., 2007). In a separate study, we expressed and purified *A. oryzae* AgtA (homologous to *A. nidulans* AmyD) in *Pichia pastoris*, and the purified *A. oryzae* AgtA showed α -amylase (hydrolysis and transferase) activity toward pNP- α -maltopentaoside (Koizumi et al., unpublished). Therefore, we evaluated the α -amylase activity in culture supernatants with pNP- α -maltopentaoside. Whereas, the hydrolysis product of pNP- α -maltopentaoside was hardly detected in Δ *amyD* (Supplementary Figure 9B), the supernatant from Δ *amyD-amyD*^{OE} (Δ GPI) produced pNP- α -maltoside and pNP- α -maltooctoside at an early stage of the reaction (Supplementary Figure 9B). These results suggest that enzymatically active AmyD that is secreted into the culture supernatant cannot decrease the amount and MM of α -1,3-glucan. Taken together, the results show that expression of AmyD with a GPI anchor is important for reaching the substrate, α -1,3-glucan, in the space of the cell wall.

Cell-wall polysaccharides are thought to be synthesized on the plasma membrane after the secretory vesicles containing polysaccharide synthases have been exported to the hyphal tip (Riquelme, 2013). On the basis of our previous findings (Miyazawa et al., 2020), we hypothesize the process of alkali-soluble glucan biosynthesis of *A. nidulans* to be as follows: (1) the intracellular domain of α -1,3-glucan synthase polymerizes 1,3-linked α -glucan chains from UDP-glucose as a substrate from the primers, which are maltooligosaccharides produced by intracellular α -amylase AmyG; (2) the elongated glucan chain is exported to the extracellular space through the multitransmembrane domain of α -1,3-glucan synthase; (3) the extracellular domain of α -1,3-glucan connects several chains of the elongated glucan to form mature alkali-soluble glucan. The mechanism underlying the distribution of mature alkali-soluble glucan to the cell-wall network is still unknown. However, the water solubility of newly synthesized glucan might be related to the spatial distribution of α -1,3-glucan in the cell wall, because localization of α -1,3-glucan varies according to the difference in MM (Miyazawa et al., 2018). *Aspergillus niger* AgtA (encoded by an ortholog of *A. nidulans amyD*) scarcely hydrolyzes α -1,3-glucan and shows weak hydrolytic activity to starch (Van Der Kaaij et al., 2007). Therefore, decrease of the MM of alkali-soluble glucan in the *amyD*^{OE} strain could be caused by hydrolysis of the primer/spacer residues (1,4-linked α -glucan) rather than of the 1,3-linked α -glucan region. The mechanism underlying the decrease in the amount of α -1,3-glucan by AmyD is also unknown. He et al. (2017) reported that AmyD seems to directly repress α -1,3-glucan synthesis. We suspect that AmyD with a GPI anchor on the plasma membrane binds to the spacer residues of a glucan chain that is being just synthesized by α -1,3-glucan synthase, and competitively inhibits transglycosylation by the

extracellular domain of α -1,3-glucan synthase to decrease the amount of alkali-soluble glucan in the cell wall.

The M_n of the alkali-soluble glucan from the wild-type strain was larger than that from the *agsB*^{OE}, although the alkali-soluble glucan from both strains seemed to be synthesized mainly by AgsB (Figure 4; Table 2). The M_n of the alkali-soluble glucan in the 16-h-cultured mycelia from the wild-type was similar to that from the 24-h-cultured mycelia (Supplementary Figure 6; Supplementary Table 2). α -1,3-Glucan was clearly labeled with AGBD-GFP in the wild-type strain (Figure 5). These results suggest that α -1,3-glucan was located in the outer layer of the cell wall in the wild-type strain, consistent with the localization of α -1,3-glucan synthesized by AgsB. These results imply the existence of some factor that increases the MM of α -1,3-glucan. We surmise that once a matured α -1,3-glucan molecule synthesized by AgsB is localized in the outer layer of the cell wall, macromolecules are formed by interconnecting α -1,3-glucan or connecting α -1,3-glucan to other polysaccharides, resulting in a chemically stable complex. Although the difference was not significant, the MM of Smith-degraded alkali-soluble glucan in the wild-type strain was slightly higher (Supplementary Table 4) and its GPC profile had a broader distribution (Supplementary Figure 7) than those in the *agsA*^{OE} and *agsB*^{OE} strains, implying the existence of non-Smith-degradable glycosidic bonds (i.e., β -1,3-glycosidic bond) in the alkali-soluble fraction in the wild-type strain. It is well-known that β -glucan, chitin, and galactomannan are continuously modified by hydrolase or glycosyltransferase in the cell wall (Aimanianda et al., 2017; Henry et al., 2019; Muszkieta et al., 2019). However, an enzyme that modifies α -1,3-glucan has not been reported. The recent report by Kang et al. (2018) on the cell wall architecture of *A. fumigatus* suggested the presence of a covalent bond of α -1,3-glucan to β -1,3- and β -1,4-glucan. The report by Chakraborty et al. (2021) on cell wall organization by whole-cell NMR showed that α -1,3-glucan fractionated into both alkali-soluble and -insoluble fractions for the rigid and mobile portions. An enzyme that has a role in modifying α -1,3-glucan to allow its transition into the different portions needs to be identified in the near future.

Here, we revealed that AmyD in *A. nidulans* decreased the MM of the alkali-soluble glucan composed mainly of α -1,3-glucan in the cell wall and also the amount of alkali-soluble glucan. However, a complete picture of the biosynthesis of

α -1,3-glucan has yet to be described, because the substrates or proteins associated with α -1,3-glucan synthesis have not been directly demonstrated. To unveil the true nature of the biosynthesis, further biochemical analysis of the α -1,3-glucan synthase is essential.

DATA AVAILABILITY STATEMENT

The original contributions presented in the study are included in the article/Supplementary Material, further inquiries can be directed to the corresponding author.

AUTHOR CONTRIBUTIONS

KM, AY, TN, and KA conceived and designed the experiment. KM, TY, and AT performed most experiments and analyzed the data. KM, YK, and YT performed microscopic observation. KM, AY, MS, and YY constructed fungal mutants. SK performed ¹³C NMR. AK and SY produced AGBD-GFP. AK and MO performed the enzymatic assay. KM, AY, and KA wrote the paper. KA supervised this research and acquired funding. All authors contributed to the article and approved the submitted version.

FUNDING

This work was supported by the Japan Society for Promotion of Science (JSPS) KAKENHI Grant Nos. 26292037 (KA), 18K05384 (KA), 20H02895 (KA) and 20K22773 (KM), and a Grant-in-Aid for JSPS Fellows Grant No. 18J11870 (KM). This work was also supported by the Institute for Fermentation, Osaka (Grant No. L-2018-2-014) (KA) and by the project JPNP20011 (KA), which is commissioned by the New Energy and Industrial Technology Development Organization (NEDO).

ACKNOWLEDGMENTS

We are grateful to Professor Toshikazu Komoda (Miyagi University) for the NMR.

SUPPLEMENTARY MATERIAL

The Supplementary Material for this article can be found online at: <https://www.frontiersin.org/articles/10.3389/ffunb.2021.821946/full#supplementary-material>

REFERENCES

- Aimanianda, V., Simenel, C., Garnaud, C., Clavaud, C., Tada, R., Barbin, L., et al. (2017). The dual activity responsible for the elongation and branching of β -(1,3)-glucan in the fungal cell wall. *mBio* 8, e00619–e00617. doi: 10.1128/mBio.00619-17
- Beauvais, A., Bozza, S., Knienmeyer, O., Formosa, C., Balloy, V., Henry, C., et al. (2013). Deletion of the α -(1,3)-glucan synthase genes induces a restructuring of the conidial cell wall responsible for the avirulence of *Aspergillus fumigatus*. *PLoS Pathog.* 9:e1003716. doi: 10.1371/journal.ppat.1003716
- Beauvais, A., Maubon, D., Park, S., Morelle, W., Tanguy, M., Huerre, M., et al. (2005). Two α (1-3) glucan synthases with different functions in *Aspergillus fumigatus*. *Appl. Environ. Microbiol.* 71, 1531–1538. doi: 10.1128/AEM.71.3.1531-1538.2005
- Bernard, M., and Latge, J. P. (2001). *Aspergillus fumigatus* cell wall: composition and biosynthesis. *Med. Mycol.* 39, 9–17. doi: 10.1080/mmy.39.1.9.17
- Chakraborty, A., Fernando, L. D., Fang, W., Dickwella Widanage, M. C., Wei, P., Jin, C., et al. (2021). A molecular vision of fungal cell wall organization by functional genomics and solid-state NMR. *Nat. Commun.* 12:6346. doi: 10.1038/s41467-021-26749-z
- Choma, A., Wiater, A., Komaniecka, I., Paduch, R., Pleszczyńska, M., and Szczodrak, J. (2013). Chemical characterization of a water insoluble (1 \rightarrow 3)- α -D-glucan from an alkaline extract of *Aspergillus wentii*. *Carbohydr. Polym.* 91, 603–608. doi: 10.1016/j.carbpol.2012.08.060

- Damveld, R. A., Vankuyk, P. A., Arentshorst, M., Klis, F. M., Van Den Hondel, C. A., and Ram, A. F. (2005). Expression of *agsA*, one of five 1,3- α -D-glucan synthase-encoding genes in *Aspergillus niger*, is induced in response to cell wall stress. *Fungal Genet. Biol.* 42, 165–177. doi: 10.1016/j.fgb.2004.11.006
- De Groot, P. W. J., Brandt, B. W., Horiuchi, H., Ram, A. F. J., De Koster, C. G., and Klis, F. M. (2009). Comprehensive genomic analysis of cell wall genes in *Aspergillus nidulans*. *Fungal Genet. Biol.* 46, S72–S81. doi: 10.1016/j.fgb.2008.07.022
- Dichtl, K., Samantaray, S., Amanianda, V., Zhu, Z., Prevost, M. C., Latgè, J. P., et al. (2015). *Aspergillus fumigatus* devoid of cell wall β -1,3-glucan is viable, massively sheds galactomannan and is killed by septum formation inhibitors. *Mol. Microbiol.* 95, 458–471. doi: 10.1111/mmi.12877
- Fontaine, T., Beauvais, A., Loussert, C., Thevenard, B., Fulgsang, C. C., Ohno, N., et al. (2010). Cell wall α 1-3glucans induce the aggregation of germinating conidia of *Aspergillus fumigatus*. *Fungal Genet. Biol.* 47, 707–712. doi: 10.1016/j.fgb.2010.04.006
- Fontaine, T., Simenel, C., Dubreucq, G., Adam, O., Delepierre, M., Lemoine, J., et al. (2000). Molecular organization of the alkali-insoluble fraction of *Aspergillus fumigatus* cell wall. *J. Biol. Chem.* 275, 27594–27607. doi: 10.1074/jbc.M909975199
- Fujikawa, T., Kuga, Y., Yano, S., Yoshimi, A., Tachiki, T., Abe, K., et al. (2009). Dynamics of cell wall components of *Magnaporthe grisea* during infectious structure development. *Mol. Microbiol.* 73, 553–570. doi: 10.1111/j.1365-2958.2009.06786.x
- Fujikawa, T., Sakaguchi, A., Nishizawa, Y., Kouzai, Y., Minami, E., Yano, S., et al. (2012). Surface α -1,3-glucan facilitates fungal stealth infection by interfering with innate immunity in plants. *PLoS Pathog.* 8:e1002882. doi: 10.1371/journal.ppat.1002882
- Fujioka, T., Mizutani, O., Furukawa, K., Sato, N., Yoshimi, A., Yamagata, Y., et al. (2007). MpkA-dependent and -independent cell wall integrity signaling in *Aspergillus nidulans*. *Eukaryot. Cell* 6, 1497–1510. doi: 10.1128/EC.00281-06
- Gow, N. A. R., Latge, J. P., and Munro, C. A. (2017). The fungal cell wall: structure, biosynthesis, and function. *Microbiol. Spectr.* 5:FUNK-0035-2016. doi: 10.1128/97811555819583.ch12
- Grün, C. H., Hochstenbach, F., Humbel, B. M., Verkleij, A. J., Sietsma, J. H., Klis, F. M., et al. (2005). The structure of cell wall α -glucan from fission yeast. *Glycobiology* 15, 245–257. doi: 10.1093/glycob/cwi002
- Guo, M. Q., Hu, X., Wang, C., and Ai, L. (2017). “Polysaccharides: structure and solubility,” in *Solubility of Polysaccharides*, ed Z. Xu (London: IntechOpen), 7–21.
- Hagiwara, D., Asano, Y., Marui, J., Furukawa, K., Kanamaru, K., Kato, M., et al. (2007). The SskA and SrrA response regulators are implicated in oxidative stress responses of hyphae and asexual spores in the phosphorelay signaling network of *Aspergillus nidulans*. *Biosci. Biotechnol. Biochem.* 71, 1003–1014. doi: 10.1271/bbb.60665
- He, X., Li, S., and Kaminsky, S. (2017). An amylase-like protein, AmyD, is the major negative regulator for α -glucan synthesis in *Aspergillus nidulans* during the asexual life cycle. *Int. J. Mol. Sci.* 18:695. doi: 10.3390/ijms18040695
- He, X. X., Li, S. N., and Kaminsky, S. G. W. (2014). Characterization of *Aspergillus nidulans* α -glucan synthesis: roles for two synthases and two amylases. *Mol. Microbiol.* 91, 579–595. doi: 10.1111/mmi.12480
- Henry, C., Latgè, J. P., and Beauvais, A. (2012). α 1,3 Glucans are dispensable in *Aspergillus fumigatus*. *Eukaryot. Cell* 11, 26–29. doi: 10.1128/EC.05270-11
- Henry, C., Li, J., Danion, F., Alcazar-Fuoli, L., Mellado, E., Beau, R., et al. (2019). Two KTR mannosyltransferases are responsible for the biosynthesis of cell wall mannans and control polarized growth in *Aspergillus fumigatus*. *mBio* 10, e02647–e02618. doi: 10.1128/mBio.02647-18
- Kang, X., Kirui, A., Muszynski, A., Widanage, M. C. D., Chen, A., Azadi, P., et al. (2018). Molecular architecture of fungal cell walls revealed by solid-state NMR. *Nat. Commun.* 9:2747. doi: 10.1038/s41467-018-05199-0
- Krappmann, S., Sasse, C., and Braus, G. H. (2006). Gene targeting in *Aspergillus fumigatus* by homologous recombination is facilitated in a nonhomologous end-joining-deficient genetic background. *Eukaryot. Cell* 5, 212–215. doi: 10.1128/EC.5.1.212-215.2006
- Latgè, J. P. (2010). Tasting the fungal cell wall. *Cell. Microbiol.* 12, 863–872. doi: 10.1111/j.1462-5822.2010.01474.x
- Latgè, J. P., and Beauvais, A. (2014). Functional duality of the cell wall. *Curr. Opin. Microbiol.* 20, 111–117. doi: 10.1016/j.mib.2014.05.009
- Latgè, J. P., Beauvais, A., and Chamilos, G. (2017). The cell wall of the human fungal pathogen *Aspergillus fumigatus*: biosynthesis, organization, immune response, and virulence. *Annu. Rev. Microbiol.* 71, 99–116. doi: 10.1146/annurev-micro-030117-020406
- Li, J., Mouyna, I., Henry, C., Moyrand, F., Malosse, C., Chamot-Rooke, J., et al. (2018). Glycosylphosphatidylinositol anchors from galactomannan and GPI-anchored protein are synthesized by distinct pathways in *Aspergillus fumigatus*. *J. Fungi* 4:19. doi: 10.3390/jof4010019
- Maubon, D., Park, S., Tanguy, M., Huerre, M., Schmitt, C., Prevost, M. C., et al. (2006). AGS3, an α (1-3)glucan synthase gene family member of *Aspergillus fumigatus*, modulates mycelium growth in the lung of experimentally infected mice. *Fungal Genet. Biol.* 43, 366–375. doi: 10.1016/j.fgb.2006.01.006
- Miyazawa, K., Yoshimi, A., and Abe, K. (2020). The mechanisms of hyphal pellet formation mediated by polysaccharides, α -1,3-glucan and galactosaminogalactan, in *Aspergillus* species. *Fungal Biol. Biotechnol.* 7:10. doi: 10.1186/s40694-020-00101-4
- Miyazawa, K., Yoshimi, A., Kasahara, S., Sugahara, A., Koizumi, A., Yano, S., et al. (2018). Molecular mass and localization of α -1,3-glucan in cell wall control the degree of hyphal aggregation in liquid culture of *Aspergillus nidulans*. *Front. Microbiol.* 9:2623. doi: 10.3389/fmicb.2018.02623
- Miyazawa, K., Yoshimi, A., Sano, M., Tabata, F., Sugahara, A., Kasahara, S., et al. (2019). Both galactosaminogalactan and α -1,3-glucan contribute to aggregation of *Aspergillus oryzae* hyphae in liquid culture. *Front. Microbiol.* 10:2090. doi: 10.3389/fmicb.2019.02090
- Miyazawa, K., Yoshimi, A., Zhang, S., Sano, M., Nakayama, M., Gomi, K., et al. (2016). Increased enzyme production under liquid culture conditions in the industrial fungus *Aspergillus oryzae* by disruption of the genes encoding cell wall α -1,3-glucan synthase. *Biosci. Biotechnol. Biochem.* 80, 1853–1863. doi: 10.1080/09168451.2016.1209968
- Muszkiet, L., Fontaine, T., Beau, R., Mouyna, I., Vogt, M. S., Trow, J., et al. (2019). The glycosylphosphatidylinositol-anchored DFG family is essential for the insertion of galactomannan into the β -(1,3)-glucan–chitin core of the cell wall of *Aspergillus fumigatus*. *mSphere* 4, e00397–e00319. doi: 10.1128/mSphere.00397-19
- Orlean, P. (2012). Architecture and biosynthesis of the *Saccharomyces cerevisiae* cell wall. *Genetics* 192, 775–818. doi: 10.1534/genetics.112.144485
- Puanglek, S., Kimura, S., Enomoto-Rogers, Y., Kabe, T., Yoshida, M., Wada, M., et al. (2016). *In vitro* synthesis of linear α -1,3-glucan and chemical modification to ester derivatives exhibiting outstanding thermal properties. *Sci. Rep.* 6:30479. doi: 10.1038/srep30479
- Rappleye, C. A., Eissenberg, L. G., and Goldman, W. E. (2007). *Histoplasma capsulatum* α -(1,3)-glucan blocks innate immune recognition by the β -glucan receptor. *Proc. Natl. Acad. Sci. U. S. A.* 104, 1366–1370. doi: 10.1073/pnas.0609848104
- Rappleye, C. A., Engle, J. T., and Goldman, W. E. (2004). RNA interference in *Histoplasma capsulatum* demonstrates a role for α -(1,3)-glucan in virulence. *Mol. Microbiol.* 53, 153–165. doi: 10.1111/j.1365-2958.2004.04131.x
- Riquelme, M. (2013). Tip growth in filamentous fungi: a road trip to the apex. *Annu. Rev. Microbiol.* 67, 587–609. doi: 10.1146/annurev-micro-092412-155652
- Samalova, M., Carr, P., Bromley, M., Blatzer, M., Moya-Nilges, M., Latgè, J. P., et al. (2020). GPI anchored proteins in *Aspergillus fumigatus* and cell wall morphogenesis. *Curr. Top. Microbiol. Immunol.* 425, 167–186. doi: 10.1007/82_2020_207
- Sheppard, D. C., and Howell, P. L. (2016). Biofilm exopolysaccharides of pathogenic fungi: lessons from bacteria. *J. Biol. Chem.* 291, 12529–12537. doi: 10.1074/jbc.R116.720995
- Stephen-Victor, E., Karnam, A., Fontaine, T., Beauvais, A., Das, M., Hegde, P., et al. (2017). *Aspergillus fumigatus* cell wall α -(1,3)-glucan stimulates regulatory T-cell polarization by inducing PD-L1 expression on human dendritic cells. *J. Infect. Dis.* 216, 1281–1294. doi: 10.1093/infdis/jix469
- Suyotha, W., Yano, S., Takagi, K., Rattanakit-Chandet, N., Tachiki, T., and Wakayama, M. (2013). Domain structure and function of α -1,3-glucanase from *Bacillus circulans* KA-304, an enzyme essential for degrading basidiomycete cell walls. *Biosci. Biotechnol. Biochem.* 77, 639–647. doi: 10.1271/bbb.120900
- Svensson, B. (1994). Protein engineering in the α -amylase family: catalytic mechanism, substrate specificity, and stability. *Plant Mol. Biol.* 25, 141–157. doi: 10.1007/BF00023233

- Tokashiki, J., Hayashi, R., Yano, S., Watanabe, T., Yamada, O., Toyama, H., et al. (2019). Influence of α -1,3-glucan synthase gene *agsE* on protoplast formation for transformation of *Aspergillus luchuensis*. *J. Biosci. Bioeng.* 128, 129–134. doi: 10.1016/j.jbiosc.2019.01.018
- Uechi, K., Yaguchi, H., Tokashiki, J., Taira, T., and Mizutani, O. (2021). Identification of genes involved in the synthesis of fungal cell wall component nigeran and regulation of its polymerization in *Aspergillus luchuensis*. *Appl. Environ. Microbiol.* 87:e0114421. doi: 10.1128/AEM.01144-21
- Usui, T., and Murata, T. (1988). Enzymatic synthesis of *p*-nitrophenyl α -maltopentaoside in an aqueous-methanol solvent system by maltotetraose-forming amylase: a substrate for human amylase in serum. *J. Biochem.* 103, 969–972. doi: 10.1093/oxfordjournals.jbchem.a122395
- Van Der Kaaij, R. M., Yuan, X. L., Franken, A., Ram, A. F., Punt, P. J., Van Der Maarel, M. J., et al. (2007). Two novel, putatively cell wall-associated and glycosylphosphatidylinositol-anchored α -glucanotransferase enzymes of *Aspergillus niger*. *Eukaryot. Cell* 6, 1178–1188. doi: 10.1128/EC.00354-06
- Vogt, M. S., Schmitz, G. F., Varón Silva, D., Mösch, H. U., and Essen, L. O. (2020). Structural base for the transfer of GPI-anchored glycoproteins into fungal cell walls. *Proc. Natl. Acad. Sci. U. S. A.* 117, 22061–22067. doi: 10.1073/pnas.2010661117
- Yoshimi, A., Miyazawa, K., and Abe, K. (2016). Cell wall structure and biogenesis in *Aspergillus* species. *Biosci. Biotechnol. Biochem.* 80, 1700–1711. doi: 10.1080/09168451.2016.1177446
- Yoshimi, A., Miyazawa, K., and Abe, K. (2017). Function and biosynthesis of cell wall α -1,3-glucan in fungi. *J. Fungi* 3:63. doi: 10.3390/jof3040063
- Yoshimi, A., Sano, M., Inaba, A., Kokubun, Y., Fujioka, T., Mizutani, O., et al. (2013). Functional analysis of the α -1,3-glucan synthase genes *agsA* and *agsB* in *Aspergillus nidulans*: AgsB is the major α -1,3-glucan synthase in this fungus. *PLoS ONE* 8:e54893. doi: 10.1371/journal.pone.0054893
- Zhang, S., Ban, A., Ebara, N., Mizutani, O., Tanaka, M., Shintani, T., et al. (2017a). Self-excising Cre/mutant *lox* marker recycling system for multiple gene integrations and consecutive gene deletions in *Aspergillus oryzae*. *J. Biosci. Bioeng.* 123, 403–411. doi: 10.1016/j.jbiosc.2016.11.001
- Zhang, S., Sato, H., Ichinose, S., Tanaka, M., Miyazawa, K., Yoshimi, A., et al. (2017b). Cell wall α -1,3-glucan prevents α -amylase adsorption onto fungal cell in submerged culture of *Aspergillus oryzae*. *J. Biosci. Bioeng.* 124, 47–53. doi: 10.1016/j.jbiosc.2017.02.013

Conflict of Interest: The authors declare that the research was conducted in the absence of any commercial or financial relationships that could be construed as a potential conflict of interest.

Publisher's Note: All claims expressed in this article are solely those of the authors and do not necessarily represent those of their affiliated organizations, or those of the publisher, the editors and the reviewers. Any product that may be evaluated in this article, or claim that may be made by its manufacturer, is not guaranteed or endorsed by the publisher.

Copyright © 2022 Miyazawa, Yamashita, Takeuchi, Kamachi, Yoshimi, Tashiro, Koizumi, Ogata, Yano, Kasahara, Sano, Yamagata, Nakajima and Abe. This is an open-access article distributed under the terms of the Creative Commons Attribution License (CC BY). The use, distribution or reproduction in other forums is permitted, provided the original author(s) and the copyright owner(s) are credited and that the original publication in this journal is cited, in accordance with accepted academic practice. No use, distribution or reproduction is permitted which does not comply with these terms.